

Magnetization plateau and quantum phase transition of the $S = 1/2$ trimerized XXZ spin chain

Kiyomi Okamoto[†] and Atsuhiko Kitazawa[‡]

[†]Department of Physics, Tokyo Institute of Technology, Oh-Okayama, Meguro-ku, Tokyo 152-8551, Japan

[‡]Department of Physics, Kyushu University 33, Fukuoka, 812-8581, Japan

Abstract. We study the plateau of the magnetization curve at $M = M_s/3$ (M_s is the saturation magnetization) of the $S = 1/2$ trimerized XXZ spin chain. By examining the level crossing of low-lying excitations obtained from the numerical diagonalization, we precisely determine the phase boundary between the plateau state and the no-plateau state on the $\Delta - t$ plane, where Δ denotes the XXZ anisotropy and t the magnitude of the trimerization. This quantum phase transition is of the Berezinskii-Kosterlitz-Thouless type.

PACS numbers: 75.10.Jm, 75.60.Ej, 75.40.Cx

1. Introduction

In recent years the quantized plateau of the magnetization curve of spin chains has been attracting much attention. Hida [1] numerically studied the $S = 1/2$ ferromagnetic-ferromagnetic-antiferromagnetic trimerized Heisenberg chain and found the plateau of the magnetization curve at $M = M_s/3$ (M_s is the saturation magnetization) for some parameter region of J_F/J_{AF} , where J_F and J_{AF} are the ferromagnetic and antiferromagnetic couplings, respectively. One of the present authors (K.O.) [2] analytically investigated Hida's model to clarify the mechanism for the appearance and disappearance of the $M = M_s/3$ plateau. Later related numerical and theoretical [3, 4, 5, 6, 7, 8] are reported in the literature. The magnetization plateaus are also found experimentally in $S = 1$ Ni compound $[\text{Ni}_2(\text{Medpt})_2(\mu\text{-ox})(\mu\text{-N}_3)]\text{ClO}_4 \cdot 0.5\text{H}_2\text{O}$ [9] and in $S = 1/2$ Cu compound NH_4CuCl_3 [10]. The behaviour of the magnetization curve of NH_4CuCl_3 is quite remarkable, because magnetization plateaus observed at $M = (3/4)M_s$ and $M = (1/4)M_s$ but not at $M = 0$ and $M = (1/2)M_s$.

Oshikawa, Yamanaka and Affleck [7] gave the necessary condition for the appearance of the magnetization plateau

$$n(S - \langle m \rangle) = \text{integer} \quad (1)$$

where n is the periodicity of the state, S the magnitude of spins and $\langle m \rangle$ the average magnetization per one spin. Since (1) is the necessary condition, it depends on the details of the models whether the magnetization plateau exists or not, even if the condition (1) is satisfied.

In this paper we study the $M = M_s/3$ plateau of the $S = 1/2$ trimerized XXZ spin chain described by

$$H = \sum_{j=1}^L \left\{ J' [h_{3j-2,3j-1}(\Delta) + h_{3j-2,3j-1}(\Delta)] + J h_{3j,3j+1}(\Delta) \right\} \quad (2)$$

where

$$h_{l,m}(\Delta) = S_l^x S_m^x + S_l^y S_m^y + \Delta S_l^z S_m^z. \quad (3)$$

Our model is sketched in figure 1.

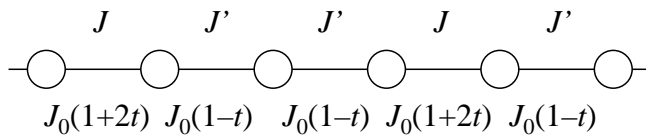


Figure 1. Sketch of the trimerized XXZ chain. The expression of the lower line corresponds to the parametrized form (4).

In §2 we qualitatively discuss the properties of the transition between the plateau and no-plateau states by use of the bosonized Hamiltonian. In §3 we determine the phase boundary of between the plateau and no-plateau states from the numerical

diagonalization data by examining the crossings of the low-lying excitations [11]. §4 is devoted to discussion.

2. Transition between the plateau state and the no-plateau state

It is convenient to parametrize the Hamiltonian (2) as

$$H = J_0 \sum_{j=1}^L \{ (1-t)[h_{3j-2,3j-1}(\Delta) + h_{3j-2,3j-1}(\Delta)] + (1+2t)h_{3j,3j+1}(\Delta) \}, \quad (4)$$

where

$$J_0 = \frac{2J' + J}{3} \quad t = -\frac{J' - J}{2J' + J}. \quad (5)$$

The model is sketched in figure 1. The bosonized expression of the Hamiltonian (4) can be obtained by the following procedure:

(a) Transforming (4) into the spinless fermion expression by use of the Jordan-Wigner transformation. The spacing between the neighboring spins is taken as the unit length.

(b) Linearizing the dispersion relation of the spinless fermions $\omega(k) = J_0 \cos k$ around $k = \pm k_F$, where $k_F \equiv \pi/3$ corresponds to the band filling of $M = M_s/3$. The Fermi velocity at $k = k_F$ is $v_F = (\sqrt{3}/2)J_0$.

(c) Taking the effects of trimerization and the interactions between fermions into account through the procedure similar to that of the standard bosonization technic.

From the above procedure, we obtain the following sine-Gordon Hamiltonian

$$H = \frac{1}{2\pi} \int dx \left[v_s K (\pi\Pi)^2 + \frac{v_s}{K} \left(\frac{\partial\phi}{\partial x} \right)^2 \right] + \frac{y_\phi v_s}{2\pi} \int dx \cos \sqrt{2}\phi \quad (6)$$

where v_s is the spin wave velocity of the system, Π is the momentum density conjugate to ϕ , $[\phi(x), \Pi(x')] = i\delta(x - x')$, and the coefficients v_s , K , and y_ϕ are related to J_0 , t and Δ as

$$v_s = \sqrt{3}J_0\sqrt{AC} \quad K = \frac{1}{2\pi}\sqrt{\frac{C}{A}} \quad y_\phi v_s = 2\pi J_0 t \quad (7)$$

where

$$A = \frac{1}{8\pi} \left(1 + \frac{5}{\sqrt{3}\pi} \Delta \right) \quad C = 2\pi \left(1 - \frac{1}{\sqrt{3}\pi} \Delta \right). \quad (8)$$

The dual field θ is defined by $\partial_x \theta = \pi\Pi$, and we make the identification $\phi \equiv \phi + \sqrt{2}\pi$, $\theta \equiv \theta + \sqrt{2}\pi$. We note that the umklapp term (which exists in $M = 0$ case and is important to describe the transition between the spin-fluid state and the Néel state) does not exist, because $2k_F$ is not equal to the reciprocal lattice wave numbers. The field ϕ is related to the fast varying (in space) part of the spin density $S^z(x)$ in the continuum picture as

$$S_{\text{fast}}^z(x) = \frac{1}{3} \left\{ \cos \left(2k_F x - \frac{\pi}{3} + \sqrt{2}\phi \right) + \frac{1}{2} \right\} \quad (9)$$

which makes it clear the physical meaning of ϕ . We note that the slowly varying part of the spin density is proportional to $\partial\phi/\partial x$.

As is well known, the excitation spectrum of the sine-Gordon model is either massive or massless depending on the values of K and y_ϕ . In the massive case the $M_s/3$ magnetization plateau exists, and in the massless case it does not [2]. It is convenient to discuss the properties of (6) in the framework of the renormalization group method. The renormalization group equations for (6) are

$$\frac{dK(L)^{-1}}{d \ln L} = \frac{1}{8}y_\phi(L)^2 \quad \frac{dy_\phi(L)}{d \ln L} = \left(2 - \frac{K(L)}{2}\right)y_\phi(L) \quad (10)$$

where L is an infrared cutoff. Denoting $K(L) = 4(1 + y_0(L)/2)$ near $K(L) = 4$, we obtain

$$\frac{dy_0(L)}{d \ln L} = -y_\phi(L)^2 \quad \frac{dy_\phi(L)}{d \ln L} = -y_0(L)y_\phi(L) \quad (11)$$

and show its flow diagram in figure 2. The Berezinskii-Kosterlitz-Thouless (BKT)

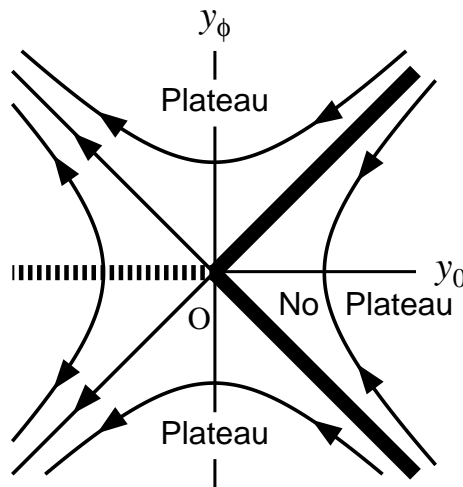


Figure 2. Flow diagram of the renormalization group equation (11). The thick solid lines show the BKT lines and the thick dotted line the Gaussian line.

transition occurs at $y_0 = |y_\phi|$, shown by thick solid lines. At the BKT transition point, by substituting $y_0 = |y_\phi|$ into equation (11), we have

$$y_0(L) = \frac{y_0}{y_0 \ln(L/L_0) + 1} \quad (12)$$

where y_0 is the bare value. When $y_0 < 0$ (*i.e.*, $K < 4$), any small (but not equal to zero) amount of trimerization brings about the magnetization plateau. The phase boundary between two plateau regions is Gaussian line (thick dotted line), on which the critical exponents vary continuously. In the no-plateau region, the effect of the trimerization vanishes in the sense of the renormalization group due to the strong quantum fluctuations.

We note that it is dangerous to apply the conventional phenomenological renormalization group method to the BKT transition, as is fully discussed in [12].

3. Numerical approach

The scaling dimension of the primary field $\mathcal{O}_{m,n} = \exp(m\sqrt{2}\phi + n\sqrt{2}\theta)$ for $y_\phi = 0$ is given by

$$x_{n,m} = \frac{K}{2}m^2 + \frac{1}{2K}n^2 \quad (13)$$

where n and m are integers with the periodic boundary condition (PBC). According to the finite size scaling theory by Cardy [13, 14], the excitation energy of the finite size system at a critical point is related to the scaling dimension as

$$x_{m,n}(L) = \frac{L}{2\pi v_s}(E_{m,n}(L) - E_g(L)) \quad (14)$$

where $E_g(L)$ is the ground state energy of L -spin system with PBC. Near the BKT transition ($K \approx 4$), the excitation energy is written as

$$\frac{L}{2\pi v_s}\Delta E_{m,0}(L) = 2m^2 + y_0(L)m^2 \quad (15)$$

$$\frac{L}{2\pi v_s}\Delta E_{0,n}(L) = \frac{1}{8}n^2 - y_0(L)\frac{1}{16}n^2 \quad (16)$$

for integer m, n . Thus, considering equation (12), we have the logarithmic corrections for finite size spectrum.

To determine the BKT transition point, we use the method developed by Nomura and Kitazawa [11], in which the level crossings for some excitations are used. With the twisted boundary condition (TBC) $S_{3L+1}^{x,y} = -S_1^{x,y}$, $S_{3L+1}^z = S_1^z$, the integer m in the operator $\mathcal{O}_{m,n}$ shifts to $m + 1/2$ as $\mathcal{O}_{m,n} \rightarrow \mathcal{O}_{m+1/2,n}$. For the scaling dimensions of the operators $\sqrt{2}\cos(\phi/\sqrt{2})$ and $\sqrt{2}\sin(\phi/\sqrt{2})$ we have the following finite size corrections

$$x_{1/2,0}^c(L) = \frac{1}{2} + \frac{1}{4}y_0(L) + \frac{1}{2}y_\phi(L) \quad (17)$$

$$x_{1/2,0}^s(L) = \frac{1}{2} + \frac{1}{4}y_0(L) - \frac{1}{2}y_\phi(L).$$

Note that scaling dimensions $x_{1/2,0}^{c,s}$ are not the form (15). This comes from the first order perturbation of the second term ($\cos\sqrt{2}\phi$ term) in equation (6). Denoting $y_\phi = \pm y_0(1 + w)$ where w measures the distance from the BKT transition point, we have for $y_\phi > 0$

$$x_{1/2,0}^c(L) = \frac{1}{2} + \frac{3}{4}y_0(L) \left(1 + \frac{2}{3}w\right) \quad (18)$$

$$x_{1/2,0}^s(L) = \frac{1}{2} - \frac{1}{4}y_0(L)(1 + 2w)$$

and for $y_\phi < 0$

$$x_{1/2,0}^c(L) = \frac{1}{2} - \frac{1}{4}y_0(L)(1 + 2w) \quad (19)$$

$$x_{1/2,0}^s(L) = \frac{1}{2} + \frac{3}{4}y_0(L) \left(1 + \frac{2}{3}w\right).$$

On the other hand, from equation (16) the scaling dimension of $\mathcal{O}_{0,\pm 2}$ is given by

$$x_{0,\pm 2}(L) = \frac{1}{2} - \frac{1}{4}y_0(L) \quad (20)$$

from which we see that $x_{0,\pm 2}$ and $x_{1/2,0}^{c,s}$ (s for $y_\phi > 0$ and c for $y_\phi < 0$) cross linearly at the transition point ($w = 0$).

In order to identify the excitation with those of the sine-Gordon model (6), we can use the following symmetry. The Hamiltonian with PBC is invariant under the spin rotation around the S^z axis, the translation by three sites, ($\mathbf{S}_j \rightarrow \mathbf{S}_{j+3}$), and space inversion ($\mathbf{S}_j \rightarrow \mathbf{S}_{L-j+1}$). Corresponding eigenvalues are M , the wave number q , and $P = \pm 1$. The space inversion in the sine-Gordon model are

$$\phi \rightarrow -\phi \quad \theta \rightarrow \theta + \pi/\sqrt{2} \quad x \rightarrow -x. \quad (21)$$

The magnetization M is related to n as $n = M_s/3 - M$. The ‘‘ground state’’ energy E_g is the lowest one with $[M = M_s/3, q = 0, P = 1]$.

In our model, the energy level corresponding to the operator $\mathcal{O}_{0,\pm 2}$ is $E_0(M_s/3 \pm 2, 0, 1)$, where $E_0(M, q, P)$ is the lowest energy with $[M, q, P]$. However, we cannot directly compare the energies with different M . In the language of the spinless fermions, the difference in M corresponds to the difference in the number of fermions, N . Thus to compare the energies with different M , we should use $E - \mu N$, where μ is the chemical potential of the spinless fermions. Since μ near $M_s/3$ is expressed as

$$\mu = \frac{1}{4} \left\{ E_0 \left(\frac{M_s}{3} + 2, 0, 1 \right) - E_0 \left(\frac{M_s}{3} - 2, 0, 1 \right) \right\} \quad (22)$$

the excitation energy corresponding to $\mathcal{O}_{0,2}$ is

$$\begin{aligned} \Delta E_{0,2} &= \left\{ E_0 \left(\frac{M_s}{3} + 2, 0, 1 \right) - E_0 \left(\frac{M_s}{3}, 0, 1 \right) - 2\mu \right\} \\ &= \frac{1}{2} \left\{ E_0 \left(\frac{M_s}{3} + 2, 0, 1 \right) + E_0 \left(\frac{M_s}{3} - 2, 0, 1 \right) \right\} - E_0 \left(\frac{M_s}{3}, 0, 1 \right). \end{aligned} \quad (23)$$

Just the same expression is obtained for $\mathcal{O}_{0,-2}$. Equation (23) can be also obtained by use of the Legendre transformation $E \rightarrow E - HM$.

The excitation energies corresponding to the operators $\sqrt{2} \cos(\phi/\sqrt{2})$ and $\sqrt{2} \sin(\phi/\sqrt{2})$ are obtained by the two lowest energies $\Delta E(M, P)$ with the twisted boundary condition as

$$\Delta E_{1/2,0}^c = E^{\text{TBC}} \left(\frac{M_s}{3}, 1 \right) - E \left(\frac{M_s}{3}, 0, 1 \right) \quad (24)$$

$$\Delta E_{1/2,0}^s = E^{\text{TBC}} \left(\frac{M_s}{3}, -1 \right) - E \left(\frac{M_s}{3}, 0, 1 \right)$$

where $E(M_s, 0, 1)$ is the lowest energy with PBC. The excitation energies $\Delta E_{0,\pm 2}$ and $\Delta E_{1/2,0}^{c,s}$ (s for $y_\phi > 0$ and c for $y_\phi < 0$) should cross linearly at the BKT transition point.

Figure 3 shows the behaviour of $\Delta E_{0,\pm 2}$ and $\Delta E_{1/2,0}^c$ for $L = 18$ spins as functions of anisotropy parameter Δ when $t = -0.25$. From the crossing point, we obtain

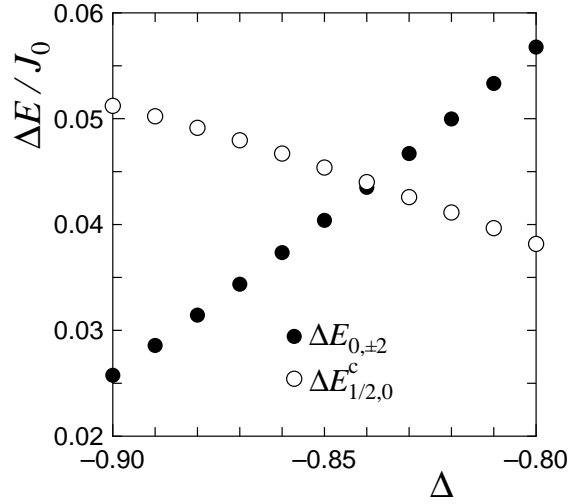


Figure 3. $\Delta E_{0,\pm 2}$ and $\Delta E_{1/2,0}^c$ for $L = 18$ spins as functions of anisotropy parameter Δ when $t = -0.25$. From the crossing point we obtain $\Delta_c(L = 18) = -0.8389$.

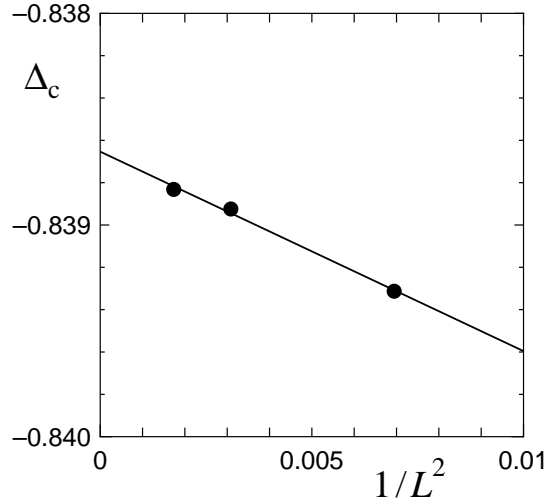


Figure 4. Extrapolation of Δ_c to $L = \infty$ when $t = -0.25$. We obtain $\Delta_c = -0.839$.

$\Delta_c = -0.8389$ for $L = 18$ spins. The BKT transition point for the infinite system can be obtained by extrapolating the Δ_c data to $L = \infty$, as shown in figure 4. Thus, we can obtain the phase diagram on the $\Delta - t$ plane as shown in figure 5. The point M ($\Delta = -0.729$) is the multicritical point where two BKT line meet together into the Gaussian line (shown by thick dotted line) on which the critical exponents vary continuously. The $\Delta \leq -1$ region is the ferromagnetic region.

Let us confirm the conformal anomaly $c = 1$ which is related to the leading finite size correction of the “ground state” energy with PBC as [15, 16]

$$E_g(L) = L\epsilon_g - \frac{\pi v_s c}{6L} + \dots \quad (25)$$

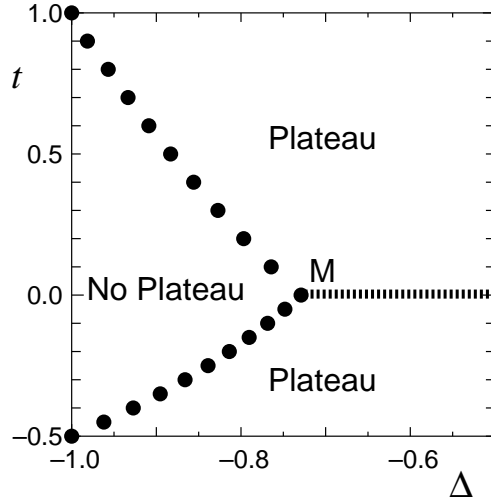


Figure 5. Phase diagram on the $\Delta - t$ plane. Closed circles are the BKT transition points determined from the numerical data as explained in the text. Thick dotted line denotes the Gaussian line. The multicritical point M corresponds to the point O of figure 2.

where ϵ_g the energy per one spin for the infinite size system. The spin wave velocity v_s can be obtained by

$$v_s = \lim_{L \rightarrow \infty} \frac{L \Delta E(q = 2\pi/L)}{2\pi} \quad (26)$$

where $\Delta E(q = 2\pi/L)$ is the lowest excitation energy having the wave number $q = 2\pi/L$ in the $M = M_s/3$ space. Thus we can check the value of c by use of equations (25) and (26). We have found that $c = 1$ is realized on the BKT line within the error of a few percent. For instance, in case of $(t, \Delta) = (0.5, -0.881)$ on the BKT line, we obtain $v_s c = 0.212J_0$ through equation (25) and $v_s = 0.217J_0$ through equation (26). Figure 6 shows the spin wave velocity v_s on the BKT transition line.

From equations (17) and (20), we can eliminate the leading logarithmic correction at the transition points ($w = 0$) using the following average

$$\frac{3x_{1/2,0}^s(L) + x_{1/2,0}^c(L)}{4} = \frac{1}{2} \quad \text{for } y_\phi > 0$$

$$\frac{3x_{1/2,0}^c(L) + x_{1/2,0}^s(L)}{4} = \frac{1}{2} \quad \text{for } y_\phi < 0. \quad (27)$$

This relation is appropriate to check our method of analyzing the numerical data. The averaged scaling dimension equation (27) on the BKT line is shown in figure 7. We can see that the averaged scaling dimension is very close to $1/2$, which guarantees the consistency of our numerical method.

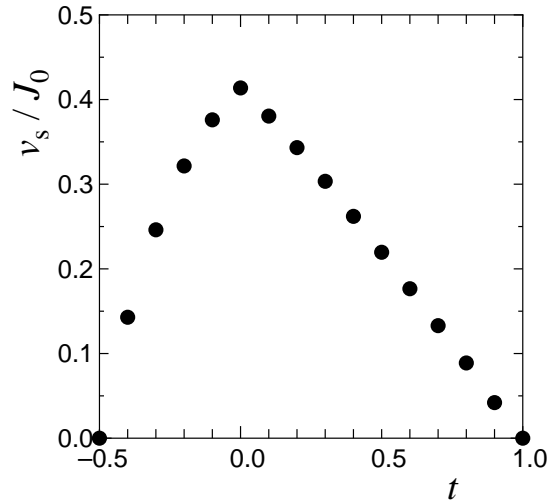


Figure 6. Spin wave velocity on the BKT line.

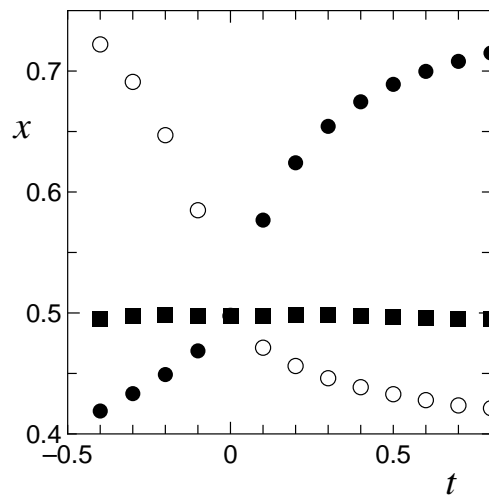


Figure 7. Scaling dimension on the BKT line. Closed circles are $x_{1/2,0}^c(L)$, open circles $x_{1/2,0}^s(L)$, and closed squares the averaged scaling dimension (27).

4. Discussion

We have obtained the phase diagram on the $\Delta - t$ plane as shown in figure 5. Two BKT lines meet together into the Gaussian line at the multicritical point M where $\Delta = \Delta_M = -0.729$. We can analytically predict the value of Δ_M from $K = 4$ with equations (7) and (8). We analytically obtain $\Delta_M = -3\sqrt{3}\pi/21 = -0.777$, which shows fairly good agreement with the numerical value. The analytically predicted value of the spin wave velocity at the multicritical point is obtained by substituting $\Delta_M = -3\sqrt{3}\pi/21$ into equation (7), which results in $v_s = 0.494J_0$.

The slopes of the BKT lines for $t > 0$ and $t < 0$ near the multicritical point M are

the same with each other. This can be explained from the symmetry of the bosonized Hamiltonian (6). Hamiltonian (6) is invariant under the transformation $t \leftrightarrow -t$ and $\sqrt{2}\phi \leftrightarrow \sqrt{2}\phi + \pi$. As the multicritical point M is gone away, on the other hand, the BKT lines on the upper and lower planes are asymmetric with each other, as can be seen from figure 5. This is quite reasonable because the $t \leftrightarrow -t$ symmetry does not hold in the original spin Hamiltonian (4). From the standpoint of the bosonized Hamiltonian, this comes from the existence of higher order terms [17] $\cos(2\sqrt{2}\phi)$, $\cos(4\sqrt{2}\phi)$, \dots , of which coefficients are also proportional to the trimerization parameter t . If these higher order terms are taken into account, the symmetry of the bosonized Hamiltonian under the transformation $t \leftrightarrow -t$ and $\sqrt{2}\phi \leftrightarrow \sqrt{2}\phi + \pi$ is lost, which explains the asymmetry of the BKT lines.

The mass-generating term $\cos(\sqrt{2}\phi)$ in the bosonized Hamiltonian (6) comes from the $J^x - J^x$ and $J^y - J^y$ couplings of the trimerization. Strictly speaking, there exists another mass-generating term

$$\frac{2t\Delta}{\pi} \int dx (\nabla\phi)^2 \cos(\sqrt{2}\phi) \quad (28)$$

which comes from the $J^z - J^z$ coupling of the trimerization. The effects of equation (28) and the $\cos(\sqrt{2}\phi)$ term in equation (6) are mutually competing when $\Delta < 0$. In the $S = 1/2$ ferromagnetic-antiferromagnetic alternating chain [18, 19], this kind of competition brings about the transition between the Haldane state and the large- D state. In our case, however, the term of equation (28) only works to reduce the coefficient of $\cos(\sqrt{2}\phi)$ in equation (6). Most simple treatment may be the approximation $(\nabla\phi)^2 \cos(\sqrt{2}\phi) \Rightarrow \langle (\nabla\phi)^2 \rangle \cos(\sqrt{2}\phi)$. In fact, we obtain the phase diagram figure 8 for the “ xy -trimerization model” in which the trimerization exists only in the $J^x - J^x$ and $J^y - J^y$ couplings and not in the $J^z - J^z$ coupling. We see that the trimerization effect is reduced in figure 5 in comparison with figure 8, because the no-plateau region is wider in figure 5 than in figure 8. We note that the phase boundary of the ferromagnetic region is no longer $\Delta = -1$, because the $SU(2)$ symmetry is broken even at $\Delta = -1$ in the xy -trimerization model. This situation is similar to the $S = 1/2$ XXZ chain under the staggered magnetic field [20]. This phase boundary can be calculated from the instability of the ferromagnetic state against the $M = M_s - 1$ spin wave excitation, resulting in

$$\Delta = -\frac{1 + 2t + \sqrt{9 - 12t + 12t^2}}{4}. \quad (29)$$

Acknowledgments

We would like to express our appreciation to K. Nomura and M. Oshikawa for fruitful discussions. A part of the numerical calculation was done by use of program package TITPACK Ver.2 coded by H. Nishimori.

References

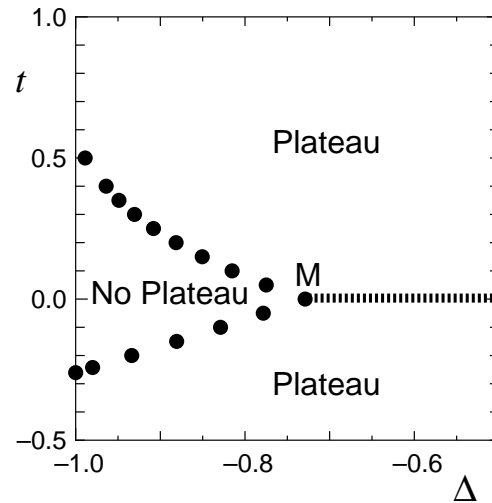


Figure 8. Phase diagram of the “ xy -trimerization model”.

- [1] Hida K 1994 *J. Phys. Soc. Jpn.* **63** 2359
- [2] Okamoto K 1996 *Solid State Commun.* **98** 245
- [3] Roji M and Miyashita S 1996 *J. Phys. Soc. Jpn.* **65** 1994
- [4] Tonegawa T, Nakao T and Kaburagi M 1996 *J. Phys. Soc. Jpn.* **65** 3317
- [5] Tonegawa T, Nishida T and Kaburagi M 1998 *Physica B* **246-247** 368
- [6] Totsuka K 1997 *Phys. Rev. B* **57** 3454
- [7] Oshikawa M, Yamanaka M and Affleck I 1997, *Phys. Rev. Lett.* **78** 1984
- [8] Sakai T and Takahashi M 1998, *Phys. Rev. B* **57** R3201
- [9] Narumi Y, Hagiwara M, Sato R, Kindo K, Nakano H and Takahashi M 1998 *Physica B* **246-247** 509
- [10] Shiramura W, Takatsu K, Kurniawan B, Tanaka H, Uekusa H, Ohashi Y, Takizawa K, Mitamura H and Goto T 1998 *J. Phys. Soc. Jpn.* **67** 1548
- [11] Nomura K and Kitazawa A 1998 *J. Phys. A: Math. Gen* **31** 7341
- [12] Okamoto K and Nomura K 1996 *J. Phys. A: Math. Gen* **26** 2279
- [13] Cardy J L 1984 *J. Phys. A: Math. Gen* **17** L385
- [14] Cardy J L 1986 *Nucl. Phys. B* **270** 186
- [15] Blöte H W J, Cardy J L and Nightingale M P 1986 *Phys. Rev. Lett* **56** 742
- [16] Affleck I 1986 *Phys. Rev. Lett.* **56** 746
- [17] Haldane F D M 1981 *Phys. Rev. Lett.* **47** 1840; (E) **48** 569
- [18] Okamoto K, Nishino D and Saika Y 1993 *J. Phys. Soc. Jpn.* **62** 2587
- [19] Okamoto K 1996 *J. Phys. A: Gen. Math.* **29** 1639
- [20] Alcaraz F C and Malveti A L 1995 *J. Phys. A: Math. Gen.* **28** 1521